



Evidence for Astrophysical Muon Neutrinos from the Northern Sky with IceCube

M. G. Aartsen,² K. Abraham,³² M. Ackermann,⁴⁸ J. Adams,¹⁵ J. A. Aguilar,¹² M. Ahlers,²⁹ M. Ahrens,³⁹ D. Altmann,²³ T. Anderson,⁴⁵ M. Archinger,³⁰ C. Argüelles,²⁹ T. C. Arlen,⁴⁵ J. Auffenberg,¹ X. Bai,³⁷ S. W. Barwick,²⁶ V. Baum,³⁰ R. Bay,⁷ J. J. Beatty,^{17,18} J. Becker Tjus,¹⁰ K.-H. Becker,⁴⁷ E. Beiser,²⁹ S. BenZvi,²⁹ P. Berghaus,⁴⁸ D. Berley,¹⁶ E. Bernardini,⁴⁸ A. Bernhard,³² D. Z. Besson,²⁷ G. Binder,^{8,7} D. Bindig,⁴⁷ M. Bissok,¹ E. Blaufuss,¹⁶ J. Blumenthal,¹ D. J. Boersma,⁴⁶ C. Bohm,³⁹ M. Börner,²⁰ F. Bos,¹⁰ D. Bose,⁴¹ S. Böser,³⁰ O. Botner,⁴⁶ J. Braun,²⁹ L. Brayeur,¹³ H.-P. Bretz,⁴⁸ A. M. Brown,¹⁵ N. Buzinsky,²² J. Casey,⁵ M. Casier,¹³ E. Cheung,¹⁶ D. Chirkin,²⁹ A. Christov,²⁴ B. Christy,¹⁶ K. Clark,⁴² L. Classen,²³ S. Coenders,³² D. F. Cowen,^{45,44} A. H. Cruz Silva,⁴⁸ J. Daughhetee,⁵ J. C. Davis,¹⁷ M. Day,²⁹ J. P. A. M. de André,²¹ C. De Clercq,¹³ H. Dembinski,³³ S. De Ridder,²⁵ P. Desiati,²⁹ K. D. de Vries,¹³ G. de Wasseige,¹³ M. de With,⁹ T. DeYoung,²¹ J. C. Díaz-Vélez,²⁹ J. P. Dumm,³⁹ M. Dunkman,⁴⁵ R. Eagan,⁴⁵ B. Eberhardt,³⁰ T. Ehrhardt,³⁰ B. Eichmann,¹⁰ S. Euler,⁴⁶ P. A. Evenson,³³ O. Fadiran,²⁹ S. Fahey,²⁹ A. R. Fazely,⁶ A. Fedynitch,¹⁰ J. Feintzeig,²⁹ J. Felde,¹⁶ K. Filimonov,⁷ C. Finley,³⁹ T. Fischer-Wasels,⁴⁷ S. Flis,³⁹ T. Fuchs,²⁰ M. Glagla,¹ T. K. Gaisser,³³ R. Gaior,¹⁴ J. Gallagher,²⁸ L. Gerhardt,^{8,7} K. Ghorbani,²⁹ D. Gier,¹ L. Gladstone,²⁹ T. Glüsenskamp,⁴⁸ A. Goldschmidt,⁸ G. Golup,¹³ J. G. Gonzalez,³³ J. A. Goodman,¹⁶ D. Göra,⁴⁸ D. Grant,²² P. Gretskov,¹ J. C. Groh,⁴⁵ A. Groß,³² C. Ha,^{8,7} C. Haack,¹ A. Haj Ismail,²⁵ A. Hallgren,⁴⁶ F. Halzen,²⁹ B. Hansmann,¹ K. Hanson,²⁹ D. Hebecker,⁹ D. Heereman,¹² K. Helbing,⁴⁷ R. Hellauer,¹⁶ D. Hellwig,¹ S. Hickford,⁴⁷ J. Hignight,²¹ G. C. Hill,² K. D. Hoffman,¹⁶ R. Hoffmann,⁴⁷ K. Holzapfel,³² A. Homeier,¹¹ K. Hoshina,^{29,*} F. Huang,⁴⁵ M. Huber,³² W. Huelsnitz,¹⁶ P. O. Hulth,³⁹ K. Hultqvist,³⁹ S. In,⁴¹ A. Ishihara,^{29,34} E. Jacobi,⁴⁸ G. S. Japaridze,⁴ K. Jero,²⁹ M. Jurkovic,³² B. Kaminsky,⁴⁸ A. Kappes,²³ T. Karg,⁴⁸ A. Karle,²⁹ M. Kauer,^{29,34} A. Keivani,⁴⁵ J. L. Kelley,²⁹ J. Kemp,¹ A. Kheirandish,²⁹ J. Kiryluk,⁴⁰ J. Kläs,⁴⁷ S. R. Klein,^{8,7} G. Kohlen,³¹ H. Kolanoski,⁹ R. Konietz,¹ A. Koob,¹ L. Köpke,³⁰ C. Kopper,²² S. Kopper,⁴⁷ D. J. Koskinen,¹⁹ M. Kowalski,^{9,48} K. Krings,³² G. Kroll,³⁰ M. Kroll,¹⁰ J. Kunnen,¹³ N. Kurahashi,³⁶ T. Kuwabara,¹⁴ M. Labare,²⁵ J. L. Lanfranchi,⁴⁵ M. J. Larson,¹⁹ M. Lesiak-Bzdak,⁴⁰ M. Leuermann,¹ J. Leuner,¹ J. Lünemann,³⁰ J. Madsen,³⁸ G. Maggi,¹³ K. B. M. Mahn,²¹ R. Maruyama,³⁴ K. Mase,¹⁴ H. S. Matis,⁸ R. Maunu,¹⁶ F. McNally,²⁹ K. Meagher,¹² M. Medici,¹⁹ A. Meli,²⁵ T. Menne,²⁰ G. Merino,²⁹ T. Meures,¹² S. Miarecki,^{8,7} E. Middell,⁴⁸ E. Middlemas,²⁹ J. Miller,¹³ L. Mohrmann,⁴⁸ T. Montaruli,²⁴ R. Morse,²⁹ R. Nahnauer,⁴⁸ U. Naumann,⁴⁷ H. Niederhausen,⁴⁰ S. C. Nowicki,²² D. R. Nygren,⁸ A. Obertacke,⁴⁷ A. Olivas,¹⁶ A. Omairat,⁴⁷ A. O'Murchadha,¹² T. Palczewski,⁴³ L. Paul,¹ J. A. Pepper,⁴³ C. Pérez de los Heros,⁴⁶ C. Pfendner,¹⁷ D. Pieloth,²⁰ E. Pinat,¹² J. Posselt,⁴⁷ P. B. Price,⁷ G. T. Przybylski,⁸ J. Pütz,¹ M. Quinnan,⁴⁵ L. Rädcl,¹ M. Rameez,²⁴ K. Rawlins,³ P. Redl,¹⁶ R. Reimann,¹ M. Relich,¹⁴ E. Resconi,³² W. Rhode,²⁰ M. Richman,³⁶ S. Richter,²⁹ B. Riedel,²² S. Robertson,² M. Rongen,¹ C. Rott,⁴¹ T. Ruhe,²⁰ B. Ruzybayev,³³ D. Ryckbosch,²⁵ S. M. Saba,¹⁰ L. Sabbatini,²⁹ H.-G. Sander,³⁰ A. Sandrock,²⁰ J. Sandroos,¹⁹ S. Sarkar,^{19,35} K. Schatto,³⁰ F. Scheriau,²⁰ M. Schimp,¹ T. Schmidt,¹⁶ M. Schmitz,²⁰ S. Schoenen,¹ S. Schöneberg,¹⁰ A. Schönwald,⁴⁸ A. Schukraft,¹ L. Schulte,¹¹ D. Seckel,³³ S. Seunarine,³⁸ R. Shanidze,⁴⁸ M. W. E. Smith,⁴⁵ D. Soldin,⁴⁷ G. M. Spiczak,³⁸ C. Spiering,⁴⁸ M. Stahlberg,¹ M. Stamatikos,^{17,†} T. Stanev,³³ N. A. Stanisha,⁴⁵ A. Stasik,⁴⁸ T. Stezelberger,⁸ R. G. Stokstad,⁸ A. Stöbl,⁴⁸ E. A. Strahler,¹³ R. Ström,⁴⁶ N. L. Strotjohann,⁴⁸ G. W. Sullivan,¹⁶ M. Sutherland,¹⁷ H. Taavola,⁴⁶ I. Taboada,⁵ S. Ter-Antonyan,⁶ A. Terliuk,⁴⁸ G. Tešić,⁴⁵ S. Tilav,³³ P. A. Toale,⁴³ M. N. Tobin,²⁹ D. Tosi,²⁹ M. Tselengidou,²³ E. Unger,⁴⁶ M. Usner,⁴⁸ S. Vallecorsa,²⁴ N. van Eijndhoven,¹³ J. Vandenbroucke,²⁹ J. van Santen,²⁹ S. Vanheule,²⁵ J. Veenkamp,³² M. Vehrung,¹ M. Voge,¹¹ M. Vraeghe,²⁵ C. Walck,³⁹ M. Wallraff,¹ N. Wandkowsky,²⁹ C. Weaver,²⁹ C. Wendt,²⁹ S. Westerhoff,²⁹ B. J. Whelan,² N. Whitehorn,²⁹ C. Wichary,¹ K. Wiebe,³⁰ C. H. Wiebusch,¹ L. Wille,²⁹ D. R. Williams,⁴³ H. Wissing,¹⁶ M. Wolf,³⁹ T. R. Wood,²² K. Woschnagg,⁷ D. L. Xu,⁴³ X. W. Xu,⁶ Y. Xu,⁴⁰ J. P. Yanez,⁴⁸ G. Yodh,²⁶ S. Yoshida,¹⁴ P. Zarzhitsky,⁴³ and M. Zoll³⁹

(IceCube Collaboration)

¹*III. Physikalisches Institut, RWTH Aachen University, D-52056 Aachen, Germany*

²*School of Chemistry and Physics, University of Adelaide, Adelaide, South Australia 5005, Australia*

³*Department of Physics and Astronomy, University of Alaska Anchorage, 3211 Providence Drive, Anchorage, Alaska 99508, USA*

⁴*CTSPS, Clark-Atlanta University, Atlanta, Georgia 30314, USA*

⁵*School of Physics and Center for Relativistic Astrophysics, Georgia Institute of Technology, Atlanta, Georgia 30332, USA*

⁶*Department of Physics, Southern University, Baton Rouge, Louisiana 70813, USA*

⁷*Department of Physics, University of California, Berkeley, California 94720, USA*

- ⁸Lawrence Berkeley National Laboratory, Berkeley, California 94720, USA
⁹Institut für Physik, Humboldt-Universität zu Berlin, D-12489 Berlin, Germany
¹⁰Fakultät für Physik and Astronomie, Ruhr-Universität Bochum, D-44780 Bochum, Germany
¹¹Physikalisches Institut, Universität Bonn, Nussallee 12, D-53115 Bonn, Germany
¹²Université Libre de Bruxelles, Science Faculty CP230, B-1050 Brussels, Belgium
¹³Vrije Universiteit Brussel, Dienst ELEM, B-1050 Brussels, Belgium
¹⁴Department of Physics, Chiba University, Chiba 263-8522, Japan
¹⁵Department of Physics and Astronomy, University of Canterbury, Private Bag 4800, Christchurch, New Zealand
¹⁶Department of Physics, University of Maryland, College Park, Maryland 20742, USA
¹⁷Department of Physics and Center for Cosmology and Astro-Particle Physics, Ohio State University, Columbus, Ohio 43210, USA
¹⁸Department of Astronomy, Ohio State University, Columbus, Ohio 43210, USA
¹⁹Niels Bohr Institute, University of Copenhagen, DK-2100 Copenhagen, Denmark
²⁰Department of Physics, TU Dortmund University, D-44221 Dortmund, Germany
²¹Department of Physics and Astronomy, Michigan State University, East Lansing, Michigan 48824, USA
²²Department of Physics, University of Alberta, Edmonton, Alberta, Canada, T6G 2E1
²³Erlangen Centre for Astroparticle Physics, Friedrich-Alexander-Universität Erlangen-Nürnberg, D-91058 Erlangen, Germany
²⁴Département de physique nucléaire et corpusculaire, Université de Genève, CH-1211 Genève, Switzerland
²⁵Department of Physics and Astronomy, University of Gent, B-9000 Gent, Belgium
²⁶Department of Physics and Astronomy, University of California, Irvine, California 92697, USA
²⁷Department of Physics and Astronomy, University of Kansas, Lawrence, Kansas 66045, USA
²⁸Department of Astronomy, University of Wisconsin, Madison, Wisconsin 53706, USA
²⁹Department of Physics and Wisconsin IceCube Particle Astrophysics Center, University of Wisconsin, Madison, Wisconsin 53706, USA
³⁰Institute of Physics, University of Mainz, Staudinger Weg 7, D-55099 Mainz, Germany
³¹Université de Mons, 7000 Mons, Belgium
³²Technische Universität München, D-85748 Garching, Germany
³³Bartol Research Institute and Department of Physics and Astronomy, University of Delaware, Newark, Delaware 19716, USA
³⁴Department of Physics, Yale University, New Haven, Connecticut 06520, USA
³⁵Department of Physics, University of Oxford, 1 Keble Road, Oxford OX1 3NP, United Kingdom
³⁶Department of Physics, Drexel University, 3141 Chestnut Street, Philadelphia, Pennsylvania 19104, USA
³⁷Physics Department, South Dakota School of Mines and Technology, Rapid City, South Dakota 57701, USA
³⁸Department of Physics, University of Wisconsin, River Falls, Wisconsin 54022, USA
³⁹Oskar Klein Centre and Department of Physics, Stockholm University, SE-10691 Stockholm, Sweden
⁴⁰Department of Physics and Astronomy, Stony Brook University, Stony Brook, New York 11794-3800, USA
⁴¹Department of Physics, Sungkyunkwan University, Suwon 440-746, Korea
⁴²Department of Physics, University of Toronto, Toronto, Ontario, Canada, M5S 1A7
⁴³Department of Physics and Astronomy, University of Alabama, Tuscaloosa, Alabama 35487, USA
⁴⁴Department of Astronomy and Astrophysics, Pennsylvania State University, University Park, Pennsylvania 16802, USA
⁴⁵Department of Physics, Pennsylvania State University, University Park, Pennsylvania 16802, USA
⁴⁶Department of Physics and Astronomy, Uppsala University, Box 516, S-75120 Uppsala, Sweden
⁴⁷Department of Physics, University of Wuppertal, D-42119 Wuppertal, Germany
⁴⁸DESY, D-15735 Zeuthen, Germany

(Received 14 May 2015; revised manuscript received 7 July 2015; published 20 August 2015)

Results from the IceCube Neutrino Observatory have recently provided compelling evidence for the existence of a high energy astrophysical neutrino flux utilizing a dominantly Southern Hemisphere data set consisting primarily of ν_e and ν_τ charged-current and neutral-current (cascade) neutrino interactions. In the analysis presented here, a data sample of approximately 35 000 muon neutrinos from the Northern sky is extracted from data taken during 659.5 days of live time recorded between May 2010 and May 2012. While this sample is composed primarily of neutrinos produced by cosmic ray interactions in Earth's atmosphere, the highest energy events are inconsistent with a hypothesis of solely terrestrial origin at 3.7σ significance. These neutrinos can, however, be explained by an astrophysical flux per neutrino flavor at a level of $\Phi(E_\nu) = 9.9^{+3.9}_{-3.4} \times 10^{-19} \text{ GeV}^{-1} \text{ cm}^{-2} \text{ sr}^{-1} \text{ s}^{-1} (E_\nu/100 \text{ TeV})^{-2}$, consistent with IceCube's Southern-Hemisphere-dominated result. Additionally, a fit for an astrophysical flux with an arbitrary spectral index is performed. We find a spectral index of $2.2^{+0.2}_{-0.2}$, which is also in good agreement with the Southern Hemisphere result.

The nature of the objects and the mechanisms which accelerate cosmic rays pose major open questions in current astrophysics, which may, in part, be answered by observations of high energy neutrinos. At high energies, the majority of cosmic rays are protons or atomic nuclei, and their interaction with other matter or radiation is known to produce neutrinos [1]. If this happens near the source of the cosmic rays, the neutrinos, which—unlike the charged cosmic rays—can travel undeflected through the magnetic fields of deep space, can point back to these sources.

IceCube is a detector constructed at depths between 1.5 and 2.5 km in glacial ice at the South Pole, instrumenting about a cubic kilometer of volume with optical sensors [2]. This forms a Cherenkov detector for the light produced when neutrinos interact and generate secondary charged particles. These interactions give rise to two characteristic event topologies: linear “tracks” produced by long-range muons emitting light as they travel and near-spherical “cascades” from the more pointlike light emission of electromagnetic and hadronic particle showers which terminate in ice after small distances compared to the instrumentation density of the detector [3].

One effective method for identifying neutrino interactions is to look for events which show no sign of light emission when entering the detector boundary. These are referred to as “starting” events. A recent IceCube study using this technique [4] has determined that astrophysical neutrinos at high energies do exist and that their flux is broadly compatible with existing models [5–7]. While such starting events provide good evidence for an astrophysical neutrino flux, they do not sample all components of the expected flux equally well. Because of absorption in Earth, few neutrinos are observed from the Northern sky, and few of the observed events are identifiably ν_μ . This analysis seeks to observe more of these particular types of events by relaxing the requirement that events begin inside the detector to permit the use of the long muon range to achieve a larger effective volume. Events are then selected based on the event topology of muons produced from ν_μ interactions to reduce background contamination. In this analysis, as in other IceCube analyses, it is not possible to distinguish neutrinos from antineutrinos, so only the combined flux can be measured.

To identify astrophysical muon neutrinos, we must distinguish them both from other types of events in the detector and from other sources of neutrinos. The majority of the data recorded by IceCube are produced by muons originating in cosmic ray air showers that penetrate the ice and reach the detector. Since this analysis seeks to take advantage of the long muon tracks and cannot depend on observing the neutrino interaction vertex inside the detector, only muons with directions that imply they passed through more material than the maximal expected muon range are selected. In this case, part of the distance must have been traversed by a neutrino, which is less prone to

interaction. This analysis accepts, therefore, only events whose reconstructed zenith angles are greater than 85° , corresponding to an overburden equivalent to at least 12 km of water. The directions of muon events are reconstructed by fitting the hypothesis of a particle moving at the speed of light and emitting Cherenkov radiation to the timing of the observed photons. The fit accounts for the expected delay of the first photon to reach each detector module due to scattering [8]. Rejecting poorly fit events removes both low energy atmospheric muons with poor direction resolution and the less numerous cascadelike events produced by neutrino interactions other than charged-current ν_μ . In addition to the direction of the muon, the other observable of interest is muon energy. A proxy for the energy is computed by fitting the amount of light expected to be emitted by a template muon to the number of observed photons in each event [9,10]. The precision of the energy proxy is limited by the relatively short section of the muon’s total track which is observed and is only loosely connected to the energy of the interacting neutrino since an unknown amount of energy is generally lost before the muon reaches the detector. After applying event-quality criteria (which are qualitatively equivalent to those used in earlier studies [11,12], with details being given in the Supplemental Material [13] and in Ref. [14]) this yields a highly pure (99.9%) sample of neutrino-induced muon events, with an efficiency of about 24% for neutrino-induced events from an E^{-2} spectrum. This selection still suffers from neutrino absorption in Earth, resulting in a loss of events at the highest zenith angles and energies. This analysis was performed with a blindness criterion such that only 10% of the experimental data were used in its development, in conjunction with simulated data, to determine the data selection. The full data were used only after the analysis technique had been fixed.

Since the astrophysical neutrinos we seek to observe in this study are expected to be produced in conjunction with the cosmic rays [15,16], they should have a related power-law spectrum of the form $\Phi \propto E^{-\gamma}$, where γ should be ~ 2 . For this analysis, we take $\gamma = 2$ as a benchmark model [17]. We also make the further simplifying assumption that the astrophysical flux is isotropic, as would be the case for a signal originating from many distant individually weak sources.

Although astrophysical neutrinos are the target of the analysis, the numerous neutrinos produced by cosmic ray air showers must be accounted for. Atmospheric neutrinos are usually separated into two groups: those produced by the decays of pions and kaons, referred to as “conventional” and those produced by the decays of heavier mesons, particularly those containing charm quarks, referred to as “prompt.” Since the conventional atmospheric neutrinos arise from relatively well-understood particle physics and have been measured by a variety of experiments [18,19], there exist several models for this flux [20–22]. Here we

use the HKKMS07 calculation [20], where the uncertainty of this calculation is estimated by its authors to be less than 10% at few GeV energies, which is consistent with measurements [23] and is expected to increase with energy to around 25% at 1 TeV. Since this model was designed for relatively low energies (100 MeV–10 TeV) compared to those considered in this analysis (~ 100 GeV–100 TeV), it is extended and modified according to the procedure in Ref. [12] to take into account the input cosmic ray spectrum [24] at high energies. An important feature of the conventional atmospheric neutrino flux is that the parent mesons may be destroyed by interactions with the medium before decaying and producing neutrinos. The energy spectrum is, therefore, steeper ($\propto E^{-3.7}$) than that of the cosmic rays from which it is produced ($\propto E^{-2.7}$) [25]. This is then markedly softer than the hypothesized spectrum of astrophysical neutrinos. The cosmic ray showering process gives these neutrinos a characteristic distribution in direction, peaked near the observer’s horizon, because of the different profiles of atmospheric density the air showers encounter.

The prompt atmospheric neutrinos are less well understood, as they have not yet been observed experimentally, and the theoretical predictions depend on understanding heavy quark production in cosmic ray-air collisions at high energies. Multiple calculations exist [26–28], and here we choose the phenomenological ERS estimate [28] of the flux, again applying corrections for the input cosmic ray spectrum. This model has a normalization uncertainty of about a factor of 2, and other calculations predict substantially larger or smaller fluxes. Like the conventional atmospheric neutrinos, the energy spectrum of the prompt component arises from the spectrum of the cosmic rays. However, since the intermediate mesons involved decay so rapidly (with a mean lifetime of 1.04×10^{-12} s for the D^\pm at rest, as opposed to 2.60×10^{-8} s for the π^\pm or 1.24×10^{-8} s for the K^\pm), losses via interactions are suppressed, and the spectrum remains similar to $E^{-2.7}$ and, likewise, remains essentially isotropic.

To fit the observed data, we implement the binned Poisson profile likelihood construction described in Ref. [11]. Here, the expected event rates for each flux component are computed by weighting a generalized simulation of neutrinos traversing Earth and interacting at IceCube according to the model’s input neutrino flux. Comparisons are made in each bin to the observed data. For this study, the data are binned in both the reconstructed zenith angle and the energy proxy. The main parameter of interest for this fit is the normalization assigned to the astrophysical flux component, while the normalizations of the background components are treated as nuisance parameters. Additional nuisance parameters include the difference between the true slope of the cosmic ray spectrum and the assumed model, the efficiency with which the IceCube hardware detects photons emitted in the ice and the relative contributions to the conventional atmospheric neutrino flux from kaon decays rather than pion decays. The nuisance parameters can be constrained using prior information from external sources, and the priors used in this analysis are listed in the fourth column of Table I.

The parameter values from fitting 659.5 days of detector live time using the benchmark set of fluxes are summarized in Table I, and the projections of the observed and fitted spectra into the reconstructed zenith angle and muon energy proxy are shown in Figs. 1 and 2, respectively [29]. The uncertainties shown for the fit parameters include both statistical and systematic contributions (at the 68% confidence level), via the profile likelihood, using the χ^2 approximation [30]. Note that the data point in Fig. 2 at muon energy proxy values of around 1.4×10^5 should not be taken as an indication of a spectral feature: a fluctuation of this size is expected to occur in approximately 9% of experiments due to statistical fluctuations, and even a delta function component in the true neutrino spectrum would be broadened into a far wider peak in the muon energy proxy [10].

TABLE I. Fit parameters are shown for two cases: when an E^{-2} astrophysical flux with equal flavor composition and equal neutrino and antineutrino components is assumed (E^{-2} fit) and when the index of the astrophysical flux is allowed to vary (best fit). The listed error ranges are 68% confidence intervals. The Gaussian priors are shown as the mean value \pm the standard deviation, but the fit results do not depend substantially on the priors. Units for the astrophysical flux normalization are $\text{GeV}^{-1} \text{cm}^{-2} \text{sr}^{-1} \text{s}^{-1}$, and HKKMS07 [20] and ERS [28] are the reference conventional and prompt atmospheric fluxes, respectively.

Parameter	E^{-2} fit	Best fit	Prior
Astrophysical flux normalization per flavor	$9.9_{-3.4}^{+3.9} \times 10^{-19}$	$1.7_{-0.8}^{+0.6} \times 10^{-18}$	≥ 0
Astrophysical flux index	Fixed to 2	$2.2_{-0.2}^{+0.2}$	None
HKKMS07 normalization	$0.93_{-0.04}^{+0.05}$	$0.93_{-0.04}^{+0.04}$	≥ 0
ERS normalization	$0.94_{-0.94}^{+1.50}$	$0^{+1.05}$	≥ 0
Cosmic ray spectral index change	$-0.024_{-0.011}^{+0.011}$	$-0.023_{-0.0008}^{+0.001}$	0 ± 0.05
Detector optical efficiency	$+9.1_{-0.5}^{+0.5}\%$	$+9.1_{-0.5}^{+0.5}\%$	None
Kaon production normalization	$1.15_{-0.07}^{+0.08}$	$1.15_{-0.07}^{+0.08}$	1 ± 0.1

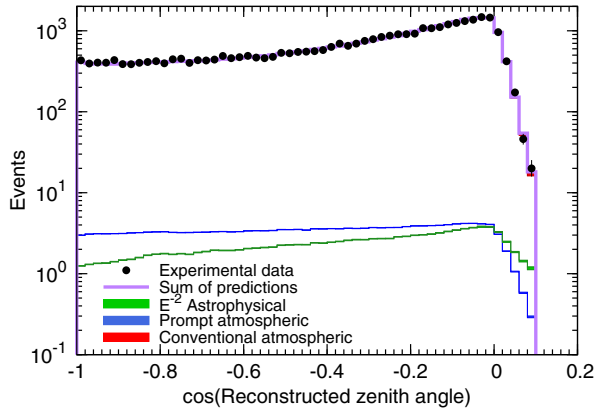


FIG. 1 (color online). The distribution of reconstructed zenith angles of events in the final sample, compared to the expected distributions for the fit of an E^{-2} astrophysical neutrino spectrum. Only statistical errors are shown, though in almost all bins they are small enough to be hidden by the data markers.

The best fit for the astrophysical component is a flux $\Phi(E_\nu) = 9.9_{-3.4}^{+3.9} \times 10^{-19} \text{ GeV}^{-1} \text{ cm}^{-2} \text{ sr}^{-1} \text{ s}^{-1} (E_\nu/100 \text{ TeV})^{-2}$ per flavor. The best-fit prompt component is 0.94 times the benchmark flux but is consistent with zero. The significance of the nonzero astrophysical flux is evaluated by a likelihood ratio test to the null hypothesis that only atmospheric neutrino fluxes are present, in which case, the fitted prompt atmospheric normalization rises to 4.0 times the ERS model. An ensemble of trials is used to establish the distribution of the likelihood ratio test statistic, yielding a p value of 1.1×10^{-4} or a single-sided significance of 3.7σ .

The range of neutrino energies in which this astrophysical flux is constrained by the data is calculated to be 330 TeV–1.4 PeV. The end points of this range are found by

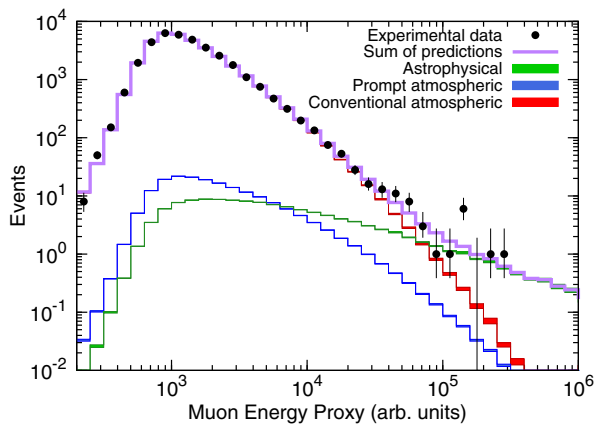


FIG. 2 (color online). The distribution of reconstructed muon energy proxy for events in the final sample, compared to the expected distributions for the fit of an E^{-2} astrophysical neutrino spectrum. Only statistical errors are shown. The energy proxy does not have a linear relationship to actual muon energy, but values $\sim 3 \times 10^3$ are roughly equivalent to the same quantity in GeV. Larger proxy values increasingly tend to underestimate muon energies, while smaller values tend to overestimate.

applying a hard cutoff to one end of the astrophysical flux template, refitting the data with the other astrophysical flux parameters held constant, and moving the cutoff inward until the resulting fit likelihood is 0.5σ worse than the best fit. This gives a conservative estimate of the energy range in which the astrophysical flux is necessary to explain the observed data, although the flux may actually have a greater extent [31]. The flux should not be interpreted as existing strictly within this energy range; were this the case, simulation trials suggest that this analysis would measure a flux normalization only 5%–20% of the result shown in Table I.

Since the true flux need not have a spectral index of exactly 2, the fit was repeated allowing the index to vary, leading to a result of $\Phi(E_\nu) = 1.7_{-0.8}^{+0.6} \times 10^{-18} \text{ GeV}^{-1} \text{ cm}^{-2} \text{ sr}^{-1} \text{ s}^{-1} (\frac{E_\nu}{100 \text{ TeV}})^{-2.2 \pm 0.2}$. The nuisance parameters do not change significantly, except for the prompt atmospheric normalization, which falls to zero, as shown in Table I. Figure 3 shows the confidence regions for the astrophysical flux normalization and spectral index and compares this result to three other IceCube analyses using starting events [4,32,33]. The compatibility of these results is noteworthy because this work uses an independent set of data from the others (a single, near-horizontal, high energy track event is shared with the other samples), while the starting event results are highly correlated with each other. The spectral indices found by this work and by the starting event analyses are consistent within their respective uncertainties, but the best-fit spectrum for this data set is slightly harder than those for the starting event analyses, particularly those extending to lower energies, which are uniquely able to probe nonatmospheric contributions to the neutrino flux. A single power law provides an acceptable fit to all data; however, the present data cannot yet rule out

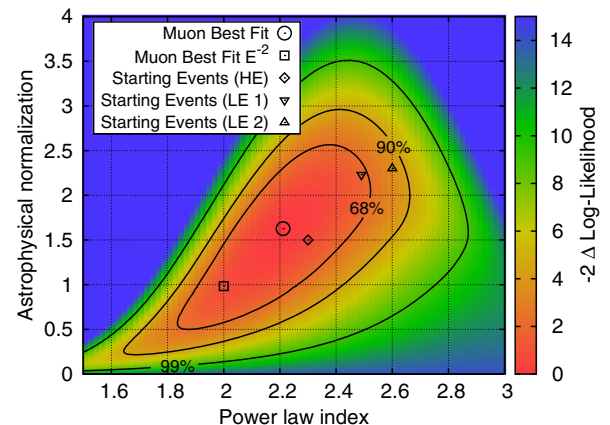


FIG. 3 (color online). Likelihood profile of the astrophysical flux power-law index and the flux normalization at 100 TeV in units of $10^{-18} \text{ GeV}^{-1} \text{ cm}^{-2} \text{ sr}^{-1} \text{ s}^{-1}$. While the E^{-2} result is well within the 68% contour, it is not the overall best fit. Also shown are the best fits from various IceCube analyses of starting events, which generally have good agreement: Starting Events (HE) [4], Starting Events (LE 1) [32], Starting Events (LE 2) [33].

the possibility that the astrophysical neutrino flux is not isotropic or that the spectrum is not a pure power law.

In this study, we see a clear excess of data above the expected atmospheric neutrino backgrounds at high energies, similar to the result of Ref. [4]. In particular, despite the fact that these are almost entirely disjoint data sets (a single, near-horizontal track event, event 5 from Ref. [4], appears in both samples), both excesses are consistent in normalization within uncertainties, assuming an E^{-2} spectrum: $9.5 \pm 3 \times 10^{-19} \text{ GeV}^{-1} \text{ cm}^{-2} \text{ sr}^{-1} \text{ s}^{-1}$ from the starting event study and $9.9_{-3.4}^{+3.9} \times 10^{-19} \text{ GeV}^{-1} \text{ cm}^{-2} \text{ sr}^{-1} \text{ s}^{-1}$ from this work. These measurements do use different calculations of the neutrino-nucleon cross sections, which influence the conversion of the flux into a rate of observed events: the starting event study used the calculation of Ref. [34], while this study uses the updated calculation from Ref. [35], which differs by 5%–10% at the energies relevant to these analyses, but this is a relatively small effect compared to the uncertainties of these results. Thus, the observed data are found to be consistent with a flux consisting of equal parts of all neutrino flavors. Similar consistency is seen in a recent analysis of starting events [33]. As shown in Fig. 3, the results for arbitrary power laws are also in good agreement. These two measurements are compared in Fig. 4, along with other recent measurements and theoretical models. The result of this study also suggests that astrophysical neutrinos are present at the several hundred TeV energies where observations were lacking in the data set of Ref. [4], suggesting that this was merely a statistical fluctuation.

Models of the astrophysical neutrino flux besides unbroken power laws can also be considered. Here we examine a small number of representative models. One candidate

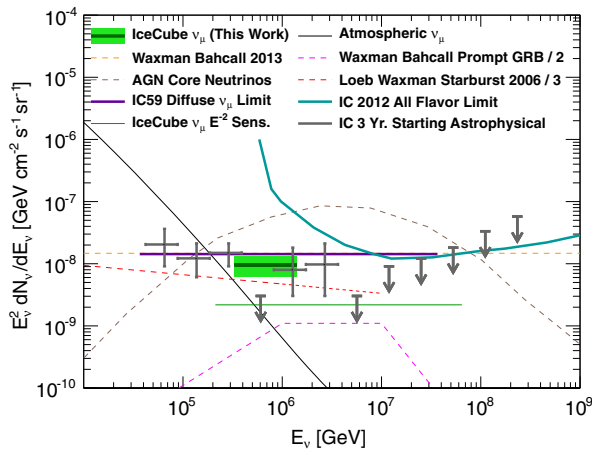


FIG. 4 (color online). Comparison of the best-fit per-flavor astrophysical flux spectrum of E^{-2} from this work, assuming a flavor ratio of 1:1:1 (shown in dark green with the 68% error range in lighter green) to other selected IceCube measurements (heavy lines) [4,12] and theoretical model predictions (thin dashed lines) [5–7,17,20,28]. The sensitivity of this analysis is also shown as the thin green line.

source type is the cores of active galactic nuclei (AGN) [6,36–39]. A fit of the AGN flux model [6] to the data in this analysis demonstrates an incompatibility in the normalization, with the predicted flux being too large by a factor of 6. Another possible source class is regions with high star formation including starburst galaxies [5,40–44]. Comparing the $E^{-2.15}$ spectrum proposed by Ref. [5] to the data reported here, we find that it is compatible after its normalization is multiplied by a factor of 2.5. Finally, gamma ray bursts (GRBs) have been long considered candidates for neutrino production [7,45–48], but recent dedicated searches by IceCube for neutrinos correlated with GRBs have placed strong limits disfavoring this hypothesis [49].

While this work represents the first strong evidence for an astrophysical ν_μ flux in the Northern Hemisphere, the sources producing these neutrinos remain unknown. Although muon events in IceCube have subdegree angular resolution, recent IceCube searches for pointlike and extended sources of muon neutrinos found no statistically significant evidence for event clustering or correlation of neutrinos with known astrophysical objects [50]. In the Northern Hemisphere, the point source flux upper limits are 10–100 times lower than the total diffuse flux level observed here, so the flux cannot originate from a small number of sources without violating those limits. The constraint on the number of sources was explored with a simple simulation where sources were injected uniformly over the Northern sky, with fluxes at the maximum levels allowed by the point source upper limit at each selected point, until the total flux reached the measured diffuse flux. On average, at least 70 sources are required to maintain consistency with the point source upper limits. This assumes each source is a true point source and emits an unbroken $E^{-2.2}$ power-law flux. If the sources instead follow harder E^{-2} power-law spectra, the diffuse flux could be split across an average of ~ 40 sources while remaining consistent with the point source analysis. Given that the diffuse flux in the Southern Hemisphere is observed at a similar flux level, this observation suggests that the flux has a large isotropic component dominated by a large population of extragalactic sources, although local sources can still have significant contributions.

We acknowledge the support from the following agencies: U.S. National Science Foundation-Office of Polar Programs, U.S. National Science Foundation-Physics Division, University of Wisconsin Alumni Research Foundation, the Grid Laboratory of Wisconsin (GLOW) grid infrastructure at the University of Wisconsin–Madison, the Open Science Grid (OSG) grid infrastructure; U.S. Department of Energy, and National Energy Research Scientific Computing Center, the Louisiana Optical Network Initiative (LONI) grid computing resources; Natural Sciences and Engineering Research Council of Canada, WestGrid and Compute/Calcul Canada; Swedish Research Council, Swedish Polar Research Secretariat,

Swedish National Infrastructure for Computing (SNIC), and Knut and Alice Wallenberg Foundation, Sweden; German Ministry for Education and Research (BMBF), Deutsche Forschungsgemeinschaft (DFG), Helmholtz Alliance for Astroparticle Physics (HAP), Research Department of Plasmas with Complex Interactions (Bochum), Germany; Fund for Scientific Research (FNRS-FWO), FWO Odysseus programme, Flanders Institute to encourage scientific and technological research in industry (IWT), Belgian Federal Science Policy Office (Belspo); University of Oxford, United Kingdom; Marsden Fund, New Zealand; Australian Research Council; Japan Society for Promotion of Science (JSPS); the Swiss National Science Foundation (SNSF), Switzerland; National Research Foundation of Korea (NRF); Danish National Research Foundation, Denmark (DNRF).

* Also at Earthquake Research Institute, University of Tokyo, Bunkyo, Tokyo 113-0032, Japan.

† Also at NASA Goddard Space Flight Center, Greenbelt, MD 20771, USA.

- [1] F. W. Stecker, *Astrophys. J.* **228**, 919 (1979).
- [2] R. Abbasi *et al.* (IceCube Collaboration), *Nucl. Instrum. Methods Phys. Res., Sect. A* **601**, 294 (2009).
- [3] A. Achterberg *et al.* (IceCube Collaboration), *Astropart. Phys.* **26**, 155 (2006).
- [4] M. G. Aartsen *et al.* (IceCube Collaboration), *Phys. Rev. Lett.* **113**, 101101 (2014).
- [5] A. Loeb and E. Waxman, *J. Cosmol. Astropart. Phys.* **05** (2006) 003.
- [6] F. W. Stecker, *Phys. Rev. D* **72**, 107301 (2005).
- [7] E. Waxman and J. Bahcall, *Phys. Rev. Lett.* **78**, 2292 (1997).
- [8] J. Ahrens *et al.* (AMANDA Collaboration), *Nucl. Instrum. Methods Phys. Res., Sect. A* **524**, 169 (2004).
- [9] M. G. Aartsen *et al.* (IceCube Collaboration), *J. Instrum.* **9**, P03009 (2014).
- [10] The performance of the energy reconstruction used in this analysis is shown in Fig. 22 of Ref. [9] and is discussed in Ref. [13].
- [11] R. Abbasi *et al.* (IceCube Collaboration), *Phys. Rev. D* **84**, 082001 (2011).
- [12] M. G. Aartsen *et al.* (IceCube Collaboration), *Phys. Rev. D* **89**, 062007 (2014).
- [13] See the Supplemental Material at <http://link.aps.org/supplemental/10.1103/PhysRevLett.115.081102> for details of the data selection criteria used in this work.
- [14] C. Weaver, Ph.D. thesis, University of Wisconsin, Madison, 2015.
- [15] M. Gupta and W. R. Webber, *Astrophys. J.* **340**, 1124 (1989).
- [16] J. J. Engelmann, P. Ferrando, A. Soutoul, P. Goret, and E. Juliusson, *Astron. Astrophys.* **233**, 96 (1990).
- [17] E. Waxman, [arXiv:1312.0558](https://arxiv.org/abs/1312.0558).
- [18] K. Daum *et al.* (Fréjus Collaboration), *Z. Phys. C* **66**, 417 (1995).
- [19] R. Wendell *et al.* (Super-Kamiokande Collaboration), *Phys. Rev. D* **81**, 092004 (2010).
- [20] M. Honda, T. Kajita, K. Kasahara, and S. Midorikawa, *Phys. Rev. D* **70**, 043008 (2004).
- [21] G. D. Barr, T. K. Gaisser, P. Lipari, S. Robbins, and T. Stanev, *Phys. Rev. D* **70**, 023006 (2004).
- [22] A. Fedynitch, J. Becker Tjus, and P. Desiati, *Phys. Rev. D* **86**, 114024 (2012).
- [23] M. Fechner *et al.* (Super-Kamiokande Collaboration), *Phys. Rev. D* **79**, 112010 (2009).
- [24] T. K. Gaisser, *Astropart. Phys.* **35**, 801 (2012).
- [25] T. K. Gaisser, *Cosmic Rays and Particle Physics* (Cambridge University Press, Cambridge, England, 1990).
- [26] M. Thunman, G. Ingelman, and P. Gondolo, *Astropart. Phys.* **5**, 309 (1996).
- [27] A. D. Martin, M. G. Ryskin, and A. M. Stasto, *Acta Phys. Pol. B* **34**, 3273 (2003).
- [28] R. Enberg, M. H. Reno, and I. Sarcevic, *Phys. Rev. D* **78**, 043005 (2008); see [arXiv:1502.01076](https://arxiv.org/abs/1502.01076) for an updated version of this work.
- [29] Event data can be found at <http://icecube.wisc.edu/science/data>.
- [30] S. S. Wilks, *Ann. Math. Stat.* **9**, 60 (1938).
- [31] It should be noted that the method of this calculation differs from that used in Ref. [12]. There, the calculation was of the energy range in which the analysis would theoretically be sensitive to a flux, which is independent of the observed data. The equivalent sensitive range of this analysis using the technique in Ref. [12] is found to be 212 TeV–64.5 PeV.
- [32] M. G. Aartsen *et al.* (IceCube Collaboration), *Phys. Rev. D* **91**, 022001 (2015).
- [33] M. G. Aartsen *et al.* (IceCube Collaboration), *Phys. Rev. Lett.* **114**, 171102 (2015).
- [34] A. Cooper-Sarkar and S. Sarkar, *J. High Energy Phys.* **01** (2008) 075.
- [35] A. Cooper-Sarkar, P. Mertsch, and S. Sarkar, *J. High Energy Phys.* **08** (2011) 42.
- [36] L. Nellen, K. Mannheim, and P. L. Biermann, *Phys. Rev. D* **47**, 5270 (1993).
- [37] J. Alvarez-Muñiz and P. Mészáros, *Phys. Rev. D* **70**, 123001 (2004).
- [38] K. Mannheim, T. Stanev, and P. L. Biermann, *Astron. Astrophys.* **260**, L1 (1992).
- [39] J. P. Rachen and P. Mészáros, *Phys. Rev. D* **58**, 123005 (1998).
- [40] H.-N. He, T. Wang, Y.-Z. Fan, S.-M. Liu, and D.-M. Wei, *Phys. Rev. D* **87**, 063011 (2013).
- [41] L. A. Anchordoqui, T. C. Paul, L. H. M. da Silva, D. F. Torres, and B. J. Vlcek, *Phys. Rev. D* **89**, 127304 (2014).
- [42] N. Senno, P. Mszros, K. Murase, P. Baerwald, and M. J. Rees, *Astrophys. J.* **806**, 24 (2015).
- [43] R.-Y. Liu, X.-Y. Wang, S. Inoue, R. Crocker, and F. Aharonian, *Phys. Rev. D* **89**, 083004 (2014).
- [44] S. Chakraborty and I. Izaguirre, *Phys. Lett. B* **745**, 35 (2015).
- [45] K. Murase and K. Ioka, *Phys. Rev. Lett.* **111**, 121102 (2013).
- [46] S. Ando and J. F. Beacom, *Phys. Rev. Lett.* **95**, 061103 (2005).
- [47] K. Murase and S. Nagataki, *Phys. Rev. D* **73**, 063002 (2006).
- [48] P. Baerwald, S. Himmer, and W. Winter, *Astropart. Phys.* **35**, 508 (2012).
- [49] R. Abbasi *et al.* (IceCube Collaboration), *Nature (London)* **484**, 351 (2012).
- [50] M. G. Aartsen *et al.* (IceCube Collaboration), *Astrophys. J.* **796**, 109 (2014).